

Journal Pre-proofs

Discovery of novel pyrazoline derivatives containing methyl-1*H*-indole moiety as potential inhibitors for blocking APC-Asef interactions

Peng-Fei Qi, Li Fang, Hua Li, Shu-Kai Li, Yu-Shun Yang, Jin-Liang Qi, Chen Xu, Hai-Liang Zhu

PII: S0045-2068(19)31867-X
DOI: <https://doi.org/10.1016/j.bioorg.2020.103838>
Reference: YBIOO 103838

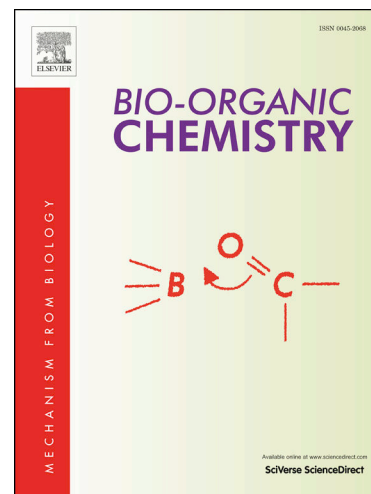
To appear in: *Bioorganic Chemistry*

Received Date: 2 November 2019
Revised Date: 1 March 2020
Accepted Date: 6 April 2020

Please cite this article as: P-F. Qi, L. Fang, H. Li, S-K. Li, Y-S. Yang, J-L. Qi, C. Xu, H-L. Zhu, Discovery of novel pyrazoline derivatives containing methyl-1*H*-indole moiety as potential inhibitors for blocking APC-Asef interactions, *Bioorganic Chemistry* (2020), doi: <https://doi.org/10.1016/j.bioorg.2020.103838>

This is a PDF file of an article that has undergone enhancements after acceptance, such as the addition of a cover page and metadata, and formatting for readability, but it is not yet the definitive version of record. This version will undergo additional copyediting, typesetting and review before it is published in its final form, but we are providing this version to give early visibility of the article. Please note that, during the production process, errors may be discovered which could affect the content, and all legal disclaimers that apply to the journal pertain.

© 2020 Published by Elsevier Inc.



Discovery of novel pyrazoline derivatives containing methyl-1*H*-indole moiety as potential inhibitors for blocking APC-Asef interactions

Peng-Fei Qi,[†] Li Fang,[†] Hua Li, Shu-Kai Li, Yu-Shun Yang, Jin-Liang Qi,^{*} Chen Xu,^{*} and

Hai-Liang Zhu^{*}

State Key Laboratory of Pharmaceutical Biotechnology, Nanjing University, Nanjing 210023, China

[†]Both authors contributed equally to the work

^{*}Corresponding author. Tel. & Fax: +86-25-89682672; E-mail: zhuhl@nju.edu.cn; xuchn@nju.edu.cn; QiJL@nju.edu.cn.

Abstract: A series of novel pyrazoline derivatives containing methyl-1*H*-indole moiety were discovered as potential inhibitors for blocking APC-Asef interactions. The top hit **Q19** suggested potency of inhibiting APC-Asef interactions and attractive preference for human-sourced colorectal cells. It was already comparable with the previous representative and the positive control Regorafenib before further pharmacokinetic optimization. The introduction of methyl-1*H*-indole moiety realized the Mitochondrial affection thus might connect the impact on the protein-interaction level with the apoptosis events. The molecular docking simulation inferred that bringing trifluoromethyl groups seemed a promising approach for causing more key interactions such as H-bonds. This work raised referable information for further discovery of inhibitors for blocking APC-Asef interactions.

Keywords: anti-cancer; pyrazoline derivatives; methyl-1*H*-indole moiety; APC-Asef interactions; molecular docking.

1. Introduction

Focusing on the topic of anti-cancer agents and therapies, researchers have been attracted by Protein-protein interactions (PPIs) due to their regulation of proliferation and migration [1-4]. Considering the tumor classification, when we keep down-to-earth and study the colon carcinoma, we found that recent in-depth therapeutic study revealed the central role of one specific protein-protein interaction in this kind of cancer cases [5,6]. Originated from colonic epithelial cells, colon cancer would transformed into adenomatous polyps pathogenically and become infectious [7-10]. Among the corresponding pathogenical mutation processes of adenomatous polypoids, adenomatous polyposis coli (APC) is a significant suppressor protein. It consists of the *N*-terminal Armadillo (ARM) domain, the middle β -catenin binding domain, and *C*-terminal binding domain with DLG tumor-inhibiting factor [11-14]. According to clinical studies, truncated APC protein was associated with over 85% of congenital colon cancer patients and 80% of the acquired cases [15,16]. Pathological APC signaling stimulation blocked the negative regulation of Asef (the receptor of APC), leading to proliferation and migration in human colorectal cancer [17-20]. Knocking down either APC or Asef could prevent their interaction thus decrease the deterioration of colorectal cancer [21-24]. More therapeutically, investigators achieved in expressing exogenous wild-type APC gene by transfecting into pathological cell and restoring full-length APC to disrupt the Asef binding with mutant APC [25]. However, knock-down, exogenous-expression and genetic induction are difficult to control for *in vivo* approaches [26-28]. Therefore, blocking the APC-Asef interaction by small functional molecules, referring to the similar binding mechanism of drugs, has drawn the attention of researchers [29-33].

In our previous work, we have exploited some novel morpholine-containing 2H pyrazole derivatives for inhibiting APC-Asef interaction [34]. The top hit indicated attractive potency ($IC_{50} = 0.18 \pm 0.01 \mu M$). However, according to the molecular docking patterns, the introduced morpholine ring did not bring strong interactions such as H-bonds or π interactions. Moreover, since the results inferred the connection

between the bioactivity and apoptosis, here we wonder if a Mitochondria-linked moiety could provide improved potency or at least valuable information. According to virtual screening, we selected 1-methyl-1*H*-indole to replace naphthalene. With similar steric effect, this choice might improve the druggability by offering better parameters (LogP and Polar Surface Area), or at least maintain good druggability when introducing the same pharmacokinetic group. Accompanying structural changes led to a new series of candidates, among whom inhibitory hits for blocking APC-Asef interaction were picked after stepwise evaluation.

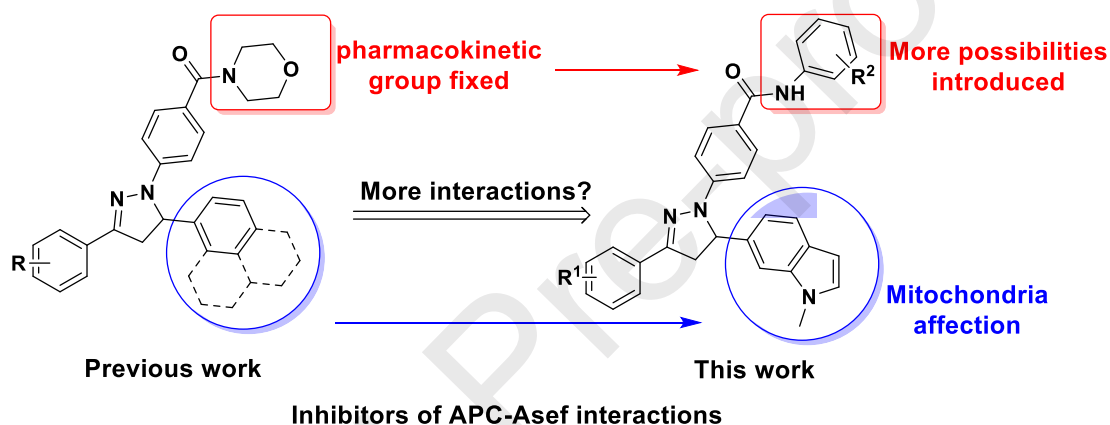


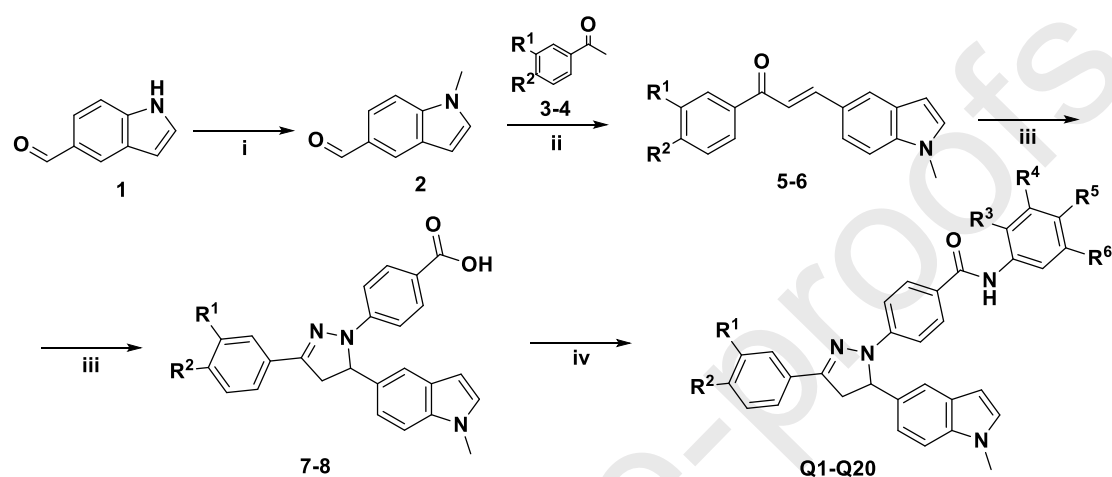
Figure 1. The designing concept of the pyrazoline derivatives containing methyl-1*H*-indole moiety as potential inhibitors for blocking APC-Asef interactions

2. Results and discussion

2.1. Synthesis of the compounds

The general synthesis route of the pyrazoline derivatives **Q1-Q20** was outlined in Scheme 1. They were prepared in four steps. First, the methylation of 1*H*-indole-5-carbaldehyde was conducted by using alkyl iodide. Second, the methylated aldehyde was treated with the corresponding acetophenones, respectively, yielding certain chalcone analogues. Third, the cyclization reaction was conducted by

using 4-hydrazinobenzoic acid. Finally, the aniline derivatives were added to achieve the target compounds **Q1-Q20**. All of them were reported for the first time with satisfactory analytical and spectroscopic data.



Compounds	R ¹	R ²	R ³	R ⁴	R ⁵	R ⁶
Q1	H	CH ₃ O	H	H	H	H
Q2	H	CH ₃ O	CH ₃ O	H	H	H
Q3	H	CH ₃ O	H	Br	H	H
Q4	H	CH ₃ O	H	H	Cl	H
Q5	H	CH ₃ O	H	H	F	H
Q6	H	CH ₃ O	CH ₃	H	H	H
Q7	H	CH ₃ O	H	Cl	Cl	H
Q8	H	CH ₃ O	H	NO ₂	NO ₂	H
Q9	H	CH ₃ O	H	CF ₃	H	CF ₃
Q10	H	CH ₃ O	H	F	F	H
Q11	CH ₃ O	H	H	H	H	H
Q12	CH ₃ O	H	CH ₃ O	H	H	H
Q14	CH ₃ O	H	H	H	Cl	H
Q15	CH ₃ O	H	H	H	F	H
Q16	CH ₃ O	H	CH ₃	H	H	H
Q17	CH ₃ O	H	H	Cl	Cl	H
Q18	CH ₃ O	H	H	H	NO ₂	H
Q19	CH ₃ O	H	H	CF ₃	H	CF ₃
Q20	CH ₃ O	H	H	F	F	H

Scheme 1. General synthesis of target compounds **Q1-Q20**. Reagents and conditions: i)

alkyl iodide, DMF, NaH, 0 °C, 30 min, r. t., 12 h; ii) acetophenone derivatives, NaOH, ethanol, r. t., 4 h; iii) CH₃COOH, methanol, 4-hydrazinobenzoic acid, reflux, 8 h; iv) aniline derivatives, EDC, HOBT, r. t., 5 h.

2.2. Biological evaluation

2.2.1. Antiproliferation assay

Initially, all the synthesized compounds **Q1-Q20** were evaluated for their antiproliferation activities against five cancer cell lines, HCT116, SW480, HT29 (human colorectal cell lines), CT26 (mice colorectal cell lines), HeLa (human cervix cell line), and one noncancer cell line, 293T (human embryonic kidney cell line). Among the human colorectal cell lines, APC is the wild type in HCT116, but the mutant ones in SW480 and HT29. According to the results of MTT assay shown in Table 1, the tested compounds seemed more potent against human-sourced colorectal cells ($GI_{50} < 10 \mu\text{M}$: 12/20 for HCT116, 3/20 for SW480, 9/20 for HT29; $GI_{50} > 30 \mu\text{M}$: 3/20 for HCT116, 8/20 for SW480, 6/20 for HT29) than either other-sourced colorectal cells ($GI_{50} < 10 \mu\text{M}$: 5/20 for CT26; $GI_{50} > 30 \mu\text{M}$: 9/20 for CT26) or human-sourced other cells ($GI_{50} < 10 \mu\text{M}$: 6/20 for HeLa; $GI_{50} > 30 \mu\text{M}$: 9/20 for HeLa). The safety could be basically ensured because the toxicity upon 293T cells was low. Among the tested cell lines, HCT116 seemed the most sensitive one to our series, which agreed with our previous study. The top hits, **Q7** ($GI_{50} = 1.95 \mu\text{M}$), **Q8** ($GI_{50} = 1.57 \mu\text{M}$), **Q19** ($GI_{50} = 1.37 \mu\text{M}$) and **Q20** ($GI_{50} = 1.98 \mu\text{M}$), all exhibited comparable potency with the positive control Regorafenib ($GI_{50} = 4.36 \mu\text{M}$).

Although this experiment was affected by the status of cells, we could still infer that this series was potential for blocking the growth of human colorectal cells. Meanwhile, the compounds did not show obvious preference for either the wild or the mutant type because their potency upon HT29 was also high.

Table1. *In vitro* antiproliferation inhibitory activity and cytotoxicity of compounds **Q1-Q20**.

Compounds	GI ₅₀ (μM)				CC ₅₀ (μM)	
	HCT116	SW480	HT29	CT26	HeLa	293T
Q1	17.8±1.19	52.4±1.21	38.8±1.92	38.3±1.15	44.3±1.69	265±7.66
Q2	20.8±1.86	43.7±1.72	30.9±1.42	19.9±0.51	27.8±1.25	130±4.14
Q3	34.2±0.96	38.6±1.44	28.8±1.16	26.8±0.73	41.8±1.36	99.3±3.77
Q4	3.17±0.61	8.83±0.70	2.33±0.46	2.80±0.21	6.61±0.56	91.2±6.35
Q5	6.06±0.73	24.2±0.93	40.2±1.17	32.6±1.41	37.8±0.97	150±12.82
Q6	11.3±1.35	38.9±1.66	68.4±1.88	71.8±1.82	53.4±1.60	144±9.66
Q7	1.95±0.48	6.76±0.17	1.82±0.49	6.36±0.36	7.59±0.83	104±8.72
Q8	1.57±0.39	29.5±0.97	3.55±0.61	9.78±0.98	4.35±0.20	92.9±7.13
Q9	3.53±0.45	4.72±0.94	2.12±0.28	7.08±0.64	3.84±0.43	178±9.60
Q10	2.41±0.94	20.7±1.16	9.75±0.74	13.0±0.87	26.8±0.90	117±7.83
Q11	13.7±1.29	21.3±1.26	27.3±1.07	42.9±1.20	18.4±0.63	103±7.99
Q12	33.9±1.23	29.8±1.38	42.4±1.49	56.9±1.46	61.9±1.72	147±6.39
Q13	31.4±1.67	36.1±1.85	24.3±0.86	27.1±0.75	43.4±1.43	89.4±5.08
Q14	9.28±1.01	29.2±1.34	2.67±0.19	8.28±0.83	9.20±0.41	137±8.25
Q15	2.49±0.36	36.9±1.45	13.5±0.29	14.9±0.56	12.8±0.13	86.8±5.06
Q16	19.3±1.96	42.1±1.64	59.4±1.72	> 200	59.5±1.95	190±15.93
Q17	2.95±0.65	25.7±1.49	1.59±0.32	15.4±0.72	4.61±0.38	142±8.93
Q18	8.47±0.89	21.5±1.36	2.03±0.16	78.76±2.24	76.3±1.76	137±7.10
Q19	1.37±0.53	10.9±0.87	1.22±0.33	46.3±1.47	19.7±0.81	119±8.30
Q20	1.98±0.57	30.3±1.94	23.5±1.48	47.6±1.31	30.2±1.15	148±5.23
Regorafenib	4.36±0.32	10.7±0.96	0.073±0.02	33.9±1.04	8.43±0.61	139±9.69

2.2.2. Blocking APC-Asef interactions

Consulting the established fluorescence polarization immunoassay to evaluate the inhibitory activity upon APC-Asef interactions [34,35], we checked the synthesized compounds in this series. The concentrations causing 50% inhibition

(IC₅₀ values) described in Table 2 indicated that some of the candidates were potential. The majority of them showed good potency with the range of IC₅₀ values varying from 1.02 to 30.5 μM. Not surprisingly, the top hits against human colorectal cells also indicated sound potency in blocking APC-Asef interactions. Therefore we could preliminarily connect the antiproliferation performance to the effect of interfering APC-Asef interactions according to their linear correlation analysis (Correlation coefficient R² = 0.8422). Generally, the difference between setting the methoxy group on R¹ or R² was not obvious. Whereas the substituent of aniline moiety suggested the preference of electron-withdrawing groups than electron-donating ones. After this stage, the most attractive hit **Q19** was selected for the following evaluation.

Table 2. Inhibitory activities of compounds **Q1-Q20** against the APC-Asef interactions

Compounds	IC ₅₀ (μM)	Compounds	IC ₅₀ (μM)
Q1	14.7±1.05	Q11	9.05±0.73
Q2	25.5±1.51	Q12	22.8±1.62
Q3	28.1±1.78	Q13	30.5±1.95
Q4	6.24±0.41	Q14	17.2±1.04
Q5	8.56±0.58	Q15	7.11±0.47
Q6	12.2±0.94	Q16	19.5±1.23
Q7	4.42±0.28	Q17	10.4±0.86
Q8	4.96±0.32	Q18	6.75±0.47
Q9	5.32±0.36	Q19	1.02±0.10
Q10	1.38±0.11	Q20	3.08±0.26

2.2.3. Apoptosis and Mitochondrial affection

Although the antiproliferation and APC-Asef interaction blocking suggested a positive correlation, there was still a long story between these two nodes. The checkpoint of apoptosis-related parameters was examined here to hint the mechanism. HCT116 cells treated with **Q19** were analyzed by flow-cytometry with Annexin V-FITC/PI system. As shown in Figure 2A, when the incubation time was set as 24 h, along with the increasing **Q19** concentrations (0, 0.20, 0.50, 1.0, 2.0, 5.0 μ M), the percentage of apoptotic cells was significantly elevated from 1.08% to 89.8%. Therefore, in dose-dependent manners, the top hit **Q19** could induce the apoptosis of human colorectal cell HCT116. Moreover, since we replaced the naphthalene with 1-methyl-1*H*-indole moiety, the Mitochondrial affection was checked here by measuring the variation of Mitochondrial membrane potential using the JC-1 assay. As shown in Figure 2B, with the dose increasing, the mitochondrial aggregate form of JC-1 gradually transferred into the monomeric form, suggesting the mitochondria depolarization of HCT116 cells. This result indicated that the introduction of 1-methyl-1*H*-indole was beneficial in the induction procedure of apoptosis between the APC-Asef interaction blocking and the antiproliferation, bringing the Mitochondrial affection as well. In Figure 2C, we used the APC-mutant HT29 cells to conduct the apoptosis assay again. **Q19** could also induce cell apoptosis in HCT29 cells in a dose-dependent manner. However, with the same time condition, the proportion of early and late apoptosis was quite different from that in HCT116 cells. This point might be further investigated when we explore the pharmacology between wt/mutant APC in future.

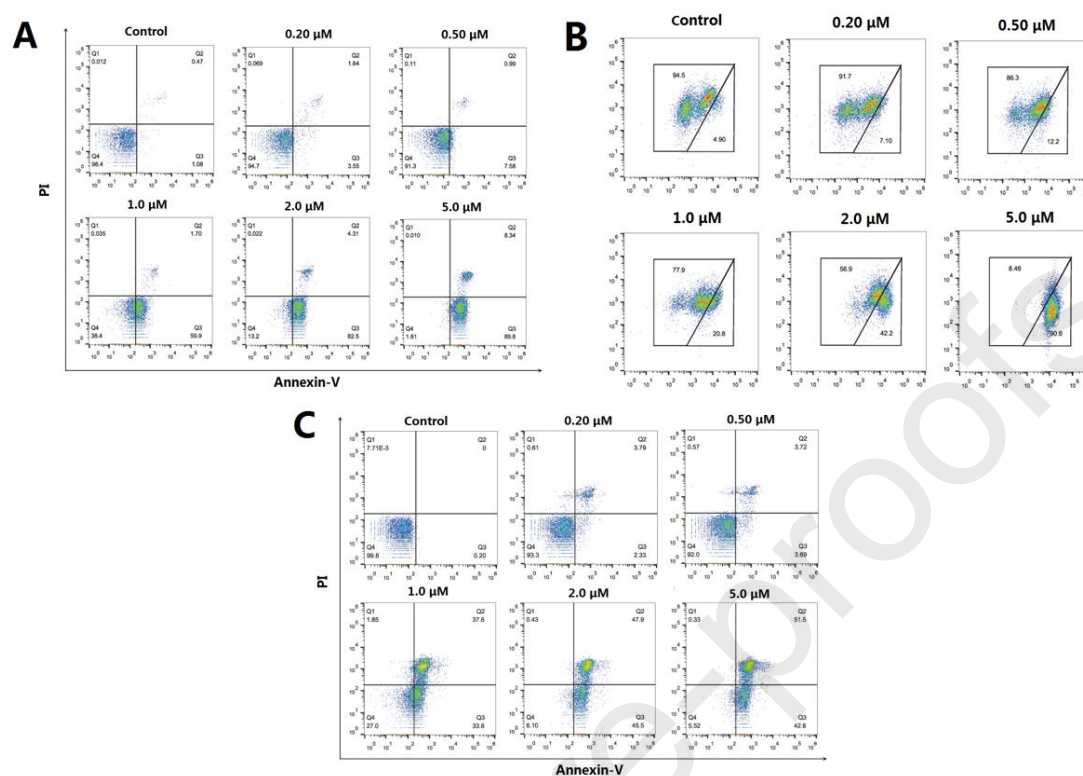


Figure 2. (A) **Q19** induced cell apoptosis in HCT116 cells in a dose-dependent manner. (B) The mitochondrial membrane potential were reduced by **Q19**. (C) **Q19** could also induce cell apoptosis in HT29 cells in a dose-dependent manner.

2.3. *In silico* study

For *in silico* study, the ADMET simulation was conducted initially to evaluate the druggability. The parameters of AlogP (the partition coefficient of drug in octanol/aqueous solution calculated by ACD/PhysChem Suite Software) and PSA_{2D} (the fast calculated polar surface area from the 2D structure) were used to predict the Absorption (human intestinal absorption) and BBB (blood-brain barrier penetration) including 95% and 99% confidence ellipses as referenced [36]. There was a major concern of this series. When we disassembled the morpholine moiety to form the

compounds in this work, whether the ADMET properties were still acceptable before regaining a pharmacokinetic group. We set three series to conduct the comparison. They were the previous series (purple) [35], the previous series with the pharmacokinetic group morpholine replaced by a simple benzene (blue), and the series in this work (reddish). In Figure 3, we could infer that although the druggability was impacted by removing the morpholine, a latter introduction of similar moieties (orange) could recover this temporary disadvantage. This kind of introduction might be conducted by rational extension on the indole ring or the methylene of pyrazoline.

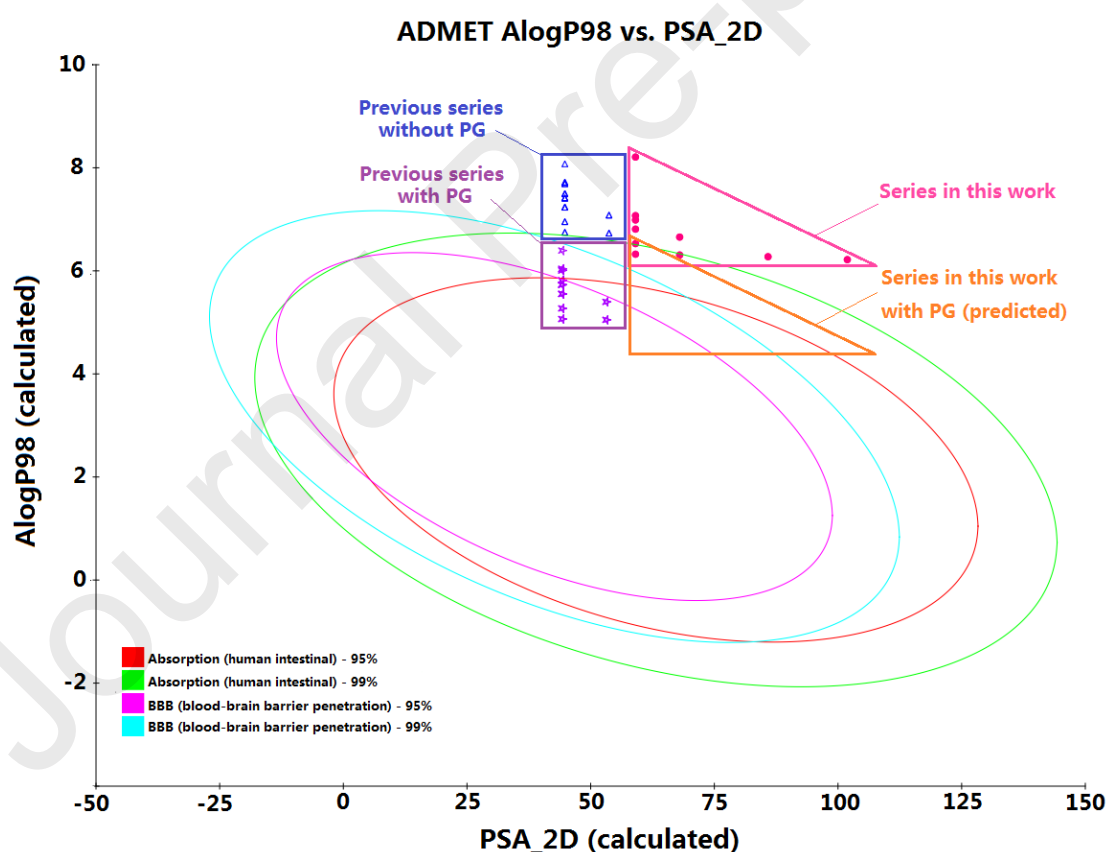


Figure 3. ADMET properties predicted for previous series and series in this work. "PG" meant "pharmacokinetic group". Plots located inside the innermost oval are better for this parameter. The percentages in the figure legend meant the 95% and 99% confidence ellipses.

The molecular docking models gave some hints for revealing the binding patterns. Since we used CDOCKER module to perform the docking simulation, the minus value of CDOCKER Interaction Energy was a crucial parameter to check the binding capability of the compounds into the binding site. In this work, the values varied within the range of 40.87-54.37 kcal/mol, which was comparable with that of the previous series ranging within 35.46-56.45 kcal/mol. The linear correlation analysis between this parameter and the APC-Asef interactions-blocking effect inferred their positive correlation (Correlation coefficient $R^2 = 0.8512$).

When we looked into the binding pattern, the result hinted possible interactions. The binding situations generally agreed with the structure-activity relationship. As the representative of this work, **Q19** indicated typical and unique interactions with several key residues on two of the three chains of APC (PDB code: 3NMX). As shown in Figure 4, two conventional hydrogen bonds (with B: Arg499 and C: Lys453) and two halogen interactions (with B: Asp539 and B: Gln542) suggested that the trifluoromethyl groups here could bring several strong binding points. These interactions could hardly be retained when trifluoromethyl groups were replaced by other options including nitro- or fluoro- groups. Among all the other interactions including π -sulfur with B: Met503, two pairs introduced by the 1-methyl-1*H*-indole were reported for the first time. The key residue, B: Lys455, participated in both the π -alkyl with and the carbon hydrogen bond. Since almost all modified moieties indicated attractive interactions, the designing strategy in this work seemed success.

The 3D and the receptor surface models also agreed with the viewpoint of raising a good binding situation.

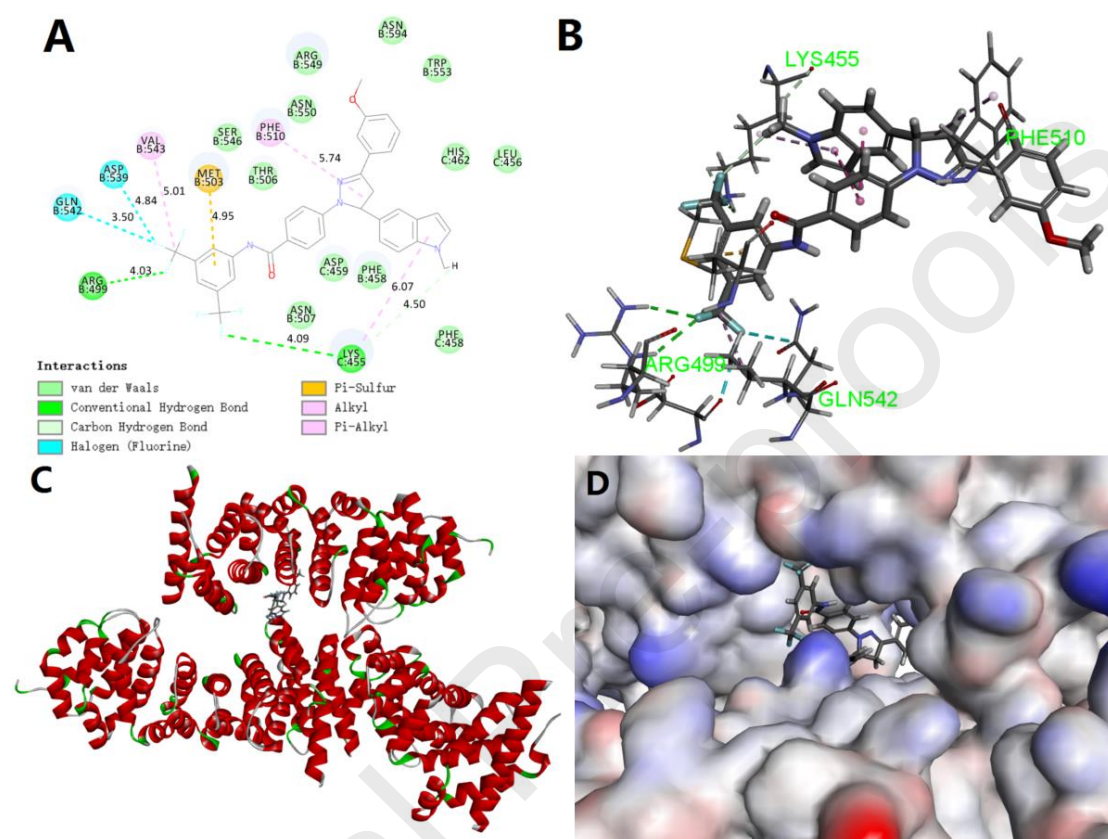


Figure 4. (A) The 2D docking pattern of representative compounds **Q19** into APC. (B) The 3D conformation of **Q19**, key residues and corresponding interactions. (C) The binding position in the whole APC protein. (D) The receptor surface model with **Q19** in APC.

3. Conclusion

In summary, this work offered the novel pyrazoline derivatives containing methyl-1*H*-indole moiety as potential inhibitors for blocking APC-Asef interactions. With the introduction of the Mitochondria-linked moiety, this series realized the Mitochondrial affection, which might connect the impact on the protein-interaction

level with the apoptosis events. The top hit **Q19** suggested potency of inhibiting APC-Asef interactions ($IC_{50} = 1.02 \mu\text{M}$) and attractive preference for human-sourced colorectal cells ($GI_{50} = 1.37 \mu\text{M}$ for HCT116; $GI_{50} = 1.22 \mu\text{M}$ for HT29). Before a further optimization with pharmacokinetic group, **Q19** was already comparable with the previous representative and the positive control Regorafenib. After bringing more possibilities with another substituent site, introducing trifluoromethyl groups seemed a promising approach for causing more key interactions such as H-bonds. With the information in this work, further researches will achieve advanced molecules with more attractive pre-clinical and even clinical potential.

4. Experimental

4.1. Materials and measurements

All chemicals (reagent grade) were purchased and used without further purification. All the NMR spectra were recorded on Bruker DPX400 or Bruker DPX600 model spectrometer in DMSO, with the chemical shifts reported as parts per million. Melting points were determined on a X4 MP apparatus (Jingsong Corp, Shanghai, China). Thin layer chromatography (TLC) was performed on the glass backed silica gel sheets (Silica Gel 60 GF254) and visualized in UV light (254 nm and 365 nm). Recombinant APC protein (HZ-APC-8) was purchased from Shanghai Huzhen Industrial Co. LTD. (Shanghai, China). APC antibody (sc-15803) and Asef anti-body (sc-13278) were purchased from Shanghai Haoran Biotechnology Co. LTD. Annexin V-FITC cell apoptosis assay kit (catalog No. BA11100) was purchased

from BIO-BOX (Nanjing, China). Matrixgel basement membrane transwell chambers were purchased from Guangzhou Hehua technology co. LTD. (Guangzhou, China).

4.2. Synthesis

Indole-5-carboxaldehyde (1.0 mmol) was dissolved in anhydrous DMF under the temperature of 0 °C. To this solution, 1.5 mmol of NaH was added portionwise and the mixture was allowed to react for 30 min. Then, 1.5 mmol of iodomethane in DMF was added dropwise and the reaction was warmed to room temperature and stirring for further 12 h. Then, reaction was quenched by 1 N HCl and washed with brine. Organic layer was separated, dried over anhydrous Na₂SO₄, filtered, and evaporated in vacuo. Crude products were purified by column chromatography using n-hexane/ethyl acetate (4:1 v:v) as mobile phase, to obtain intermediate compounds **2** with 89% of yields.

To a solution of compound **2** (6 mmol) in 10 mL absolute ethyl alcohol was added acetophenone derivatives (6 mmol) and 40% sodium hydroxide solution (9 mmol). The reaction was stirred at room temperature for 4 h and filtered to afford compounds **5-6**, which were used without further purification.

4-Hydrazinobenzoic acid (4.0 mmol), and compounds **5-6** (2.0 mmol) were dissolved in methanol, then glacial acetic acid (0.2 mmol) was added in the solution stirred at room temperature for 30 min. Then, the mixture was heated to reflux temperature and stirred overnight. The course of the reaction was checked by TLC. The crude products were purified by column chromatography using n-hexane/ethyl acetate (2:1 v:v) as eluent leading to the corresponding compounds **7-8** with 70, 68%

of yields, respectively.

To a mixture of compounds **7-8** (1 mmol) in the dichloromethane (30 mL) was added EDC (1.6 mmol), and HOBt (0.6 mmol), then the mixture was stirred at 0 °C for 30 min. Aniline derivatives (0.6 mmol) was added subsequently, and the reaction was transferred at room temperature and kept overnight. Reaction was quenched by 10% aqueous solution of sodium bicarbonate and extracted with dichloromethane. The organic layer was washed with 10% aqueous solution of sodium bicarbonate for three times, dried over anhydrous Na₂SO₄, filtered, and evaporated in vacuo. Crude products were purified by column chromatography using n-hexane/ethyl acetate (6:1 v:v) as eluent, to obtain the target compounds **Q1-Q20**.

4-(3-(4-methoxyphenyl)-5-(1-methyl-1*H*-indol-5-yl)-4,5-dihydro-1*H*-pyrazol-1-yl)-*N*-phenylbenzamide (**Q1**)

Yellow crystal, yield: 80.6%, m.p. 204-212 °C. ¹H NMR (400 MHz, DMSO-*d*₆) δ 9.82 (s, 1H), 7.76 (s, 1H), 7.74 (s, 1H), 7.71 (s, 2H), 7.69 (s, 2H), 7.46 (s, 1H), 7.39 (d, *J* = 8.4 Hz, 1H), 7.31 – 7.25 (m, 5H), 7.11 (s, 1H), 7.09 (s, 1H), 7.08-7.00 (m, 2H), 6.37 (d, *J* = 3.0 Hz, 1H), 5.67 (dd, *J* = 12.1, 5.3 Hz, 1H), 3.98 (dd, *J* = 17.7, 12.1 Hz, 1H), 3.74 (s, 3H), 3.19 (dd, *J* = 17.6, 5.4 Hz, 1H), 2.35 (s, 3H). ¹³C NMR (101 MHz, DMSO-*d*₆) δ 149.71, 140.04, 139.24, 133.08, 130.73, 129.85, 129.77, 129.35, 128.92, 128.64, 126.42, 124.15, 123.50, 120.53, 119.37, 117.92, 112.35, 110.95, 100.84, 63.51, 43.99, 32.96, 21.47. HRMS (ESI-TOF) Calcd. for C₃₂H₂₈N₄O₂ [M+H]⁺ 501.2265; Found 501.2267.

N-(4-methoxyphenyl)-4-(3-(4-methoxyphenyl)-5-(1-methyl-1*H*-indol-5-yl)-4,5-dihyd

ro-1*H*-pyrazol-1-yl)benzamide (**Q2**)

White solid, yield: 86.3%, m.p. 112-117 °C. ¹H NMR (600 MHz, DMSO-*d*₆) δ 9.00 (s, 1H), 8.14 (d, *J* = 8.4 Hz, 1H), 8.01 (d, *J* = 8.8 Hz, 1H), 7.82-7.78 (m, 1H), 7.75 (t, *J* = 9.1 Hz, 2H), 7.70 (d, *J* = 7.9 Hz, 1H), 7.62 (t, *J* = 7.7 Hz, 1H), 7.51 (t, *J* = 7.7 Hz, 1H), 7.45 (s, 1H), 7.41 (dd, *J* = 16.7, 8.5 Hz, 1H), 7.34 – 7.29 (m, 2H), 7.27 (d, *J* = 8.0 Hz, 1H), 7.10 (dd, *J* = 8.1, 5.9 Hz, 1H), 7.06 (ddt, *J* = 8.4, 4.0, 1.7 Hz, 1H), 6.95-6.90 (m, 1H), 6.38 (dd, *J* = 10.0, 3.1 Hz, 1H), 5.81 (dd, *J* = 11.8, 4.6 Hz, 1H), 4.01 (ddd, *J* = 45.2, 17.7, 12.0 Hz, 1H), 3.80 (s, 3H), 3.75 (d, *J* = 5.6 Hz, 3H), 3.22 (ddd, *J* = 53.3, 17.7, 5.0 Hz, 1H), 2.36 (d, *J* = 8.5 Hz, 3H). ¹³C NMR (151 MHz, DMSO-*d*₆) δ 150.16, 147.61, 146.83, 136.25, 133.05, 131.18, 130.76, 129.78, 129.12, 128.63, 126.48, 123.86, 123.67, 120.62, 119.85, 119.29, 117.82, 112.45, 111.59, 111.00, 100.83, 63.33, 56.12, 44.06, 32.96, 21.47. HRMS (ESI-TOF) Calcd. for C₃₃H₃₀N₄O₃ [M+H]⁺ 531.2373; Found 531.2371.

N-(3-bromophenyl)-4-(3-(4-methoxyphenyl)-5-(1-methyl-1*H*-indol-5-yl)-4,5-dihydro-1*H*-pyrazol-1-yl)benzamide (**Q3**)

White solid, yield: 76.5%, m.p. 110-115 °C. ¹H NMR (600 MHz, DMSO-*d*₆) δ 9.98 (s, 1H), 8.04 (s, 1H), 7.94 (d, *J* = 8.6 Hz, 0.5H), 7.86 (d, *J* = 7.9 Hz, 0.5H), 7.73 (dd, *J* = 19.4, 8.3 Hz, 3H), 7.68 (d, *J* = 8.4 Hz, 1H), 7.48-7.44 (m, 1H), 7.40 (d, *J* = 8.5 Hz, 1H), 7.33-7.20 (m, 5H), 7.12-7.08 (m, 2H), 7.06 (dd, *J* = 8.5, 1.4 Hz, 1H), 6.37 (d, *J* = 3.0 Hz, 1H), 5.69 (dd, *J* = 12.1, 5.3 Hz, 1H), 3.98 (dd, *J* = 17.5, 12.1 Hz, 1H), 3.81 (s, 1H), 3.74 (s, 2H), 3.19 (dd, *J* = 17.5, 5.3 Hz, 1H), 2.36 (d, *J* = 5.3 Hz, 3H). ¹³C NMR (151 MHz, DMSO-*d*₆) δ 165.77, 149.92, 146.89, 141.71, 139.31,

136.25, 133.02, 130.97, 130.76, 129.79, 129.48, 128.61, 126.46, 126.03, 123.54, 122.62, 121.80, 119.35, 119.10, 117.91, 112.36, 110.99, 100.83, 63.40, 43.95, 32.97, 21.48. HRMS (ESI-TOF) Calcd. for $C_{32}H_{27}BrN_4O_2$ $[M+H]^+$ 579.1379; Found 579.1377.

N-(4-chlorophenyl)-4-(3-(4-methoxyphenyl)-5-(1-methyl-1*H*-indol-5-yl)-4,5-dihydro-1*H*-pyrazol-1-yl)benzamide (**Q4**)

Yellow solid, yield: 60%, m.p. 142-149 °C. 1H NMR (600 MHz, DMSO- d_6) δ 8.14 (d, $J = 8.6$ Hz, 1H), 8.00 (dd, $J = 8.4, 6.4$ Hz, 2H), 7.80 (d, $J = 8.3$ Hz, 1H), 7.76 (d, $J = 8.2$ Hz, 2H), 7.64 – 7.58 (m, 1H), 7.54-7.48 (m, 1H), 7.46 (d, $J = 1.7$ Hz, 1H), 7.41 (dd, $J = 14.4, 8.5$ Hz, 2H), 7.33 (d, $J = 3.1$ Hz, 1H), 7.30 (s, 1H), 7.29 (s, 1H), 7.23 (s, 1H), 7.07 (dd, $J = 8.5, 1.8$ Hz, 1H), 6.39 (d, $J = 3.1$ Hz, 1H), 5.81 (dd, $J = 11.9, 4.6$ Hz, 1H), 4.04 (dd, $J = 17.8, 11.9$ Hz, 1H), 3.75 (s, 3H), 3.26 (dd, $J = 17.8, 4.6$ Hz, 1H), 2.36 (s, 3H). ^{13}C NMR (151 MHz, DMSO- d_6) δ 162.87, 152.65, 149.28, 143.23, 140.08, 136.34, 132.84, 132.34, 130.89, 129.87, 129.53, 129.27, 128.68, 126.86, 125.66, 120.27, 119.15, 117.73, 113.01, 111.41, 111.13, 109.77, 100.90, 63.09, 44.13, 32.98, 21.51. HRMS (ESI-TOF) Calcd. for $C_{32}H_{27}ClN_4O_2$ $[M+H]^+$ 535.1813; Found 535.1812.

N-(4-fluorophenyl)-4-(3-(4-methoxyphenyl)-5-(1-methyl-1*H*-indol-5-yl)-4,5-dihydro-1*H*-pyrazol-1-yl)benzamide (**Q5**)

White solid, yield: 83.3%, m.p. 128-135 °C. 1H NMR (600 MHz, DMSO- d_6) δ 9.68 (s, 1H), 7.97 (d, $J = 8.5$ Hz, 1H), 7.86 (d, $J = 8.0$ Hz, 1H), 7.76 (d, $J = 8.6$ Hz, 1H), 7.71 (d, $J = 8.0$ Hz, 1H), 7.62-7.57 (m, 1H), 7.54 (t, $J = 7.9$, 1H), 7.47 (dd, $J =$

8.6, 2.9 Hz, 1H), 7.45 (d, $J = 1.6$ Hz, 1H), 7.39 (d, $J = 8.0$ Hz, 1H), 7.31 (d, $J = 3.2$ Hz, 1H), 7.27 (t, $J = 6.4$ Hz, 2H), 7.23-7.20 (m, 1H), 7.17 (t, $J = 7.5, 1.7$ Hz, 1H), 7.09 (d, $J = 10.5$ Hz, 1H), 7.05 (t, $J = 9.3$ Hz, 1H), 6.37 (d, $J = 3.0$ Hz, 1H), 5.69 (dd, $J = 12.1, 5.2$ Hz, 1H), 3.98 (dd, $J = 17.6, 12.1$ Hz, 1H), 3.77 (d, $J = 39.8$ Hz, 3H), 3.19 (dd, $J = 17.6, 5.2$ Hz, 1H), 2.36 (d, $J = 6.8$ Hz, 3H). ^{13}C NMR (151 MHz, DMSO- d_6) δ 164.33, 161.80, 151.58, 148.74, 145.84, 142.16, 139.01, 135.18, 131.27, 129.81, 128.46, 127.85, 126.30, 125.55, 124.81, 124.58, 123.68, 122.50, 122.04, 119.20, 118.24, 116.79, 111.29, 110.05, 108.70, 99.75, 62.34, 43.05, 31.88, 20.40. HRMS (ESI-TOF) Calcd. for $\text{C}_{32}\text{H}_{27}\text{FN}_4\text{O}_2$ $[\text{M}+\text{H}]^+$ 519.2217; Found 519.2216.

4-(3-(4-methoxyphenyl)-5-(1-methyl-1*H*-indol-5-yl)-4,5-dihydro-1*H*-pyrazol-1-yl)-*N*-(*o*-tolyl)benzamide (**Q6**)

White solid, yield: 76.9%, m.p. 112-115 °C. ^1H NMR (600 MHz, DMSO- d_6) δ 10.13 (s, 1H), 8.18 (d, $J = 8.5$ Hz, 1H), 8.13 (d, $J = 9.1$ Hz, 2H), 8.00 (d, $J = 9.4$ Hz, 1H), 7.87 (d, $J = 8.4$ Hz, 1H), 7.83-7.80 (m, 3H), 7.67 (ddd, $J = 8.1, 6.9, 0.9$ Hz, 1H), 7.54 (ddd, $J = 8.2, 6.9, 1.0$ Hz, 1H), 7.46 (s, 1H), 7.43 (d, $J = 8.6$ Hz, 1H), 7.07 (dd, $J = 8.5, 1.8$ Hz, 1H), 7.05-7.03 (m, 1H), 7.00 (d, $J = 2.2$ Hz, 1H), 6.99 (d, $J = 2.1$ Hz, 1H), 6.39 (d, $J = 3.1$ Hz, 1H), 5.80 (td, $J = 11.6, 4.5$ Hz, 1H), 4.05 (ddd, $J = 17.6, 11.8, 5.2$ Hz, 1H), 3.82 (s, 1.5H), 3.80 (s, 3H), 3.76 (s, 1.5H), 3.26 (dd, $J = 17.8, 4.6$ Hz, 1H), 2.34 (s, 3H). ^{13}C NMR (151 MHz, DMSO- d_6) δ 165.67, 165.15, 159.91, 151.76, 149.61, 146.69, 139.03, 136.62, 134.52, 133.35, 132.96, 131.32, 130.76, 129.44, 128.85, 127.80, 127.06, 124.86, 122.30, 121.95, 119.35, 118.37, 115.50, 114.34, 112.50, 110.52, 106.60, 101.40, 100.84, 63.57, 55.65, 43.91, 32.96. HRMS (ESI-TOF)

Calcd. for $C_{33}H_{30}N_4O_2$ $[M+H]^+$ 515.2480; Found 515.2478.

N-(3,4-dichlorophenyl)-4-(3-(4-methoxyphenyl)-5-(1-methyl-1*H*-indol-5-yl)-4,5-dihydro-1*H*-pyrazol-1-yl)benzamide (**Q7**)

Yellow solid, yield: 59.8%, m.p. 114-119 °C. 1H NMR (600 MHz, DMSO- d_6) δ 8.14 (d, $J = 8.5$ Hz, 1H), 8.01 (d, $J = 9.4$ Hz, 2H), 7.81 (d, $J = 8.4$ Hz, 1H), 7.76 (d, $J = 8.2$ Hz, 2H), 7.62 (ddd, $J = 8.1, 6.9, 0.9$ Hz, 1H), 7.51 (ddd, $J = 8.2, 7.0, 1.0$ Hz, 1H), 7.46 (d, $J = 1.7$ Hz, 1H), 7.43 (d, $J = 8.5$ Hz, 1H), 7.33 (d, $J = 3.1$ Hz, 1H), 7.30 (d, $J = 8.1$ Hz, 2H), 7.23 (d, $J = 9.8$ Hz, 1H), 7.06 (dt, $J = 9.2, 2.8$ Hz, 1H), 6.39 (dd, $J = 3.1, 0.8$ Hz, 1H), 5.81 (dd, $J = 11.8, 4.6$ Hz, 1H), 4.05 (dd, $J = 17.8, 11.8$ Hz, 1H), 3.75 (d, $J = 9.6$ Hz, 3H), 3.26 (dd, $J = 17.8, 4.6$ Hz, 1H), 2.36 (s, 3H). ^{13}C NMR (151 MHz, DMSO- d_6) δ 167.71, 150.15, 147.61, 139.38, 136.25, 132.98, 131.18, 130.76, 129.78, 128.62, 128.26, 127.92, 126.48, 119.85, 119.22, 117.72, 112.34, 110.99, 109.99, 100.83, 63.33, 44.06, 32.96, 21.46. HRMS (ESI-TOF) Calcd. for $C_{32}H_{26}Cl_2N_4O_2$ $[M+H]^+$ 569.1464; Found 569.1463.

N-(3,4-dinitrophenyl)-4-(3-(4-methoxyphenyl)-5-(1-methyl-1*H*-indol-5-yl)-4,5-dihydro-1*H*-pyrazol-1-yl)benzamide (**Q8**)

White solid, yield: 85.5%, m.p. 135-142 °C. 1H NMR (600 MHz, DMSO- d_6) δ 8.14 (d, $J = 8.5$ Hz, 1H), 8.01 (s, 1H), 7.99 (s, 1H), 7.83-7.78 (m, 3H), 7.61 (t, $J = 7.6$ Hz, 1H), 7.51 (t, $J = 7.2$ Hz, 1H), 7.45 (d, $J = 1.7$ Hz, 1H), 7.43 (d, $J = 8.5$ Hz, 1H), 7.33 (d, $J = 3.1$ Hz, 1H), 7.21 (s, 1H), 7.07 (dd, $J = 8.5, 1.8$ Hz, 1H), 7.05 (s, 1H), 7.03 (s, 1H), 6.39 (dd, $J = 3.1, 0.8$ Hz, 1H), 5.79 (dd, $J = 11.8, 4.5$ Hz, 1H), 4.04 (dd, $J = 17.8, 11.8$ Hz, 1H), 3.82 (s, 3H), 3.76 (s, 3H), 3.26 (dd, $J = 17.8, 4.5$ Hz, 1H). ^{13}C

NMR (151 MHz, DMSO- d_6) δ 167.73, 160.65, 150.08, 147.70, 133.04, 131.18, 130.75, 128.62, 128.11, 125.02, 124.92, 119.76, 119.60, 119.23, 117.71, 114.66, 112.20, 110.98, 110.00, 100.83, 63.27, 55.75, 44.20, 32.96. HRMS (ESI-TOF) Calcd. for $C_{32}H_{26}N_6O_6$ $[M+H]^+$ 591.1967; Found 591.1866.

N-(3,5-bis(trifluoromethyl)phenyl)-4-(3-(4-methoxyphenyl)-5-(1-methyl-1*H*-indol-5-yl)-4,5-dihydro-1*H*-pyrazol-1-yl)benzamide (**Q9**)

White solid, yield: 90.6%, m.p. 128-140 °C. 1H NMR (600 MHz, DMSO- d_6) δ 8.14 (d, $J = 8.5$ Hz, 1H), 8.00 (d, $J = 9.3$ Hz, 2H), 7.80 (dd, $J = 8.5, 6.6$ Hz, 3H), 7.61 (ddd, $J = 8.1, 6.9, 0.9$ Hz, 1H), 7.51 (ddd, $J = 8.1, 6.9, 1.0$ Hz, 1H), 7.46 (s, 1H), 7.42 (d, $J = 8.4$ Hz, 1H), 7.33 (d, $J = 3.1$ Hz, 1H), 7.21 (s, 1H), 7.07 (dd, $J = 8.5, 1.7$ Hz, 1H), 7.05 (s, 1H), 7.03 (s, 1H), 6.40-6.35 (d, $J = 3.0$ Hz, 1H), 5.78 (dd, $J = 11.8, 4.5$ Hz, 1H), 4.03 (dd, $J = 17.8, 11.8$ Hz, 1H), 3.82 (s, 3H), 3.75 (s, 3H), 3.26 (dd, $J = 17.8, 4.5$ Hz, 1H). ^{13}C NMR (151 MHz, DMSO- d_6) δ 167.74, 162.88, 161.09, 160.64, 150.07, 149.31, 147.71, 136.25, 133.04, 132.83, 131.19, 130.88, 130.74, 129.53, 128.55, 128.27, 128.10, 125.65, 125.02, 120.27, 119.61, 119.23, 117.71, 114.74, 114.65, 112.87, 110.98, 109.77, 100.83, 63.29, 55.74, 44.20, 32.95. HRMS (ESI-TOF) Calcd. for $C_{34}H_{26}F_6N_4O_2$ $[M+H]^+$ 637.2044; Found 637.2043.

N-(3,4-difluorophenyl)-4-(3-(4-methoxyphenyl)-5-(1-methyl-1*H*-indol-5-yl)-4,5-dihydro-1*H*-pyrazol-1-yl)benzamide (**Q10**)

Yellow solid, yield: 78.2%, m.p. 130-138 °C. 1H NMR (600 MHz, DMSO- d_6) δ 8.14 (d, $J = 8.5$ Hz, 1H), 8.00 (d, $J = 8.8$ Hz, 2H), 7.80 (dd, $J = 8.4, 5.8$ Hz, 3H), 7.61 (t, $J = 7.6$ Hz, 1H), 7.51 (t, $J = 8.6$ Hz, 1H), 7.46 (s, 1H), 7.43 (d, $J = 8.5$ Hz, 1H), 7.33

(d, $J = 3.1$ Hz, 1H), 7.21 (s, 1H), 7.05 (dd, $J = 15.5, 8.7$ Hz, 3H), 6.39 (d, $J = 3.1$ Hz, 1H), 5.79 (dd, $J = 11.8, 4.5$ Hz, 1H), 4.04 (dd, $J = 17.8, 11.8$ Hz, 1H), 3.82 (s, 3H), 3.75 (s, 3H), 3.26 (dd, $J = 17.8, 4.5$ Hz, 1H). ^{13}C NMR (151 MHz, DMSO- d_6) δ 167.73, 160.64, 152.58, 150.07, 149.31, 147.71, 136.33, 136.25, 133.04, 132.83, 131.19, 130.74, 128.63, 128.56, 128.11, 125.02, 124.53, 120.27, 119.61, 119.23, 117.71, 114.65, 112.21, 111.11, 110.98, 109.77, 100.83, 63.28, 55.75, 44.20, 32.96. HRMS (ESI-TOF) Calcd. for $\text{C}_{32}\text{H}_{26}\text{F}_2\text{N}_4\text{O}_2$ $[\text{M}+\text{H}]^+$ 536.2052; Found 536.2050.

4-(3-(3-methoxyphenyl)-5-(1-methyl-1*H*-indol-5-yl)-4,5-dihydro-1*H*-pyrazol-1-yl)-*N*-phenylbenzamide (**Q11**)

White solid, yield: 85.2%, m.p. 145-150 °C ^1H NMR (600 MHz, DMSO- d_6) δ 9.85 (s, 1H), 7.75 (d, $J = 8.5$ Hz, 2H), 7.70 (d, $J = 8.0$ Hz, 2H), 7.46 (s, 1H), 7.39 (dd, $J = 16.3, 9.4$ Hz, 3H), 7.34 (s, 1H), 7.32-7.27 (m, 3H), 7.12 (d, $J = 8.5$ Hz, 2H), 7.07 (d, $J = 8.6$ Hz, 1H), 7.03 (t, $J = 7.4$ Hz, 1H), 6.99 (d, $J = 7.8$ Hz, 1H), 6.37 (d, $J = 3.0$ Hz, 1H), 5.71 (dd, $J = 12.2, 5.4$ Hz, 1H), 3.99 (dd, $J = 17.5, 12.1$ Hz, 1H), 3.83 (s, 3H), 3.74 (s, 3H), 3.22 (dd, $J = 17.6, 5.4$ Hz, 1H). ^{13}C NMR (151 MHz, DMSO- d_6) δ 165.58, 159.91, 149.50, 146.58, 140.01, 136.26, 133.92, 133.00, 130.76, 130.29, 129.37, 128.94, 128.62, 124.37, 123.53, 120.50, 119.36, 118.97, 117.92, 115.49, 112.48, 111.30, 110.98, 100.83, 63.58, 55.65, 43.91, 39.54, 32.97. HRMS (ESI-TOF) Calcd. for $\text{C}_{32}\text{H}_{28}\text{N}_4\text{O}_2$ $[\text{M}+\text{H}]^+$ 501.2325; Found 501.2325.

N-(2-methoxyphenyl)-4-(3-(3-methoxyphenyl)-5-(1-methyl-1*H*-indol-5-yl)-4,5-dihydro-1*H*-pyrazol-1-yl)benzamide (**Q12**)

White solid, yield: 93.6%, m.p. 158-163 °C ^1H NMR (600 MHz, DMSO- d_6) δ

9.01 (s, 1H), 7.81 (d, $J = 7.9$ Hz, 1H), 7.76 (d, $J = 8.6$ Hz, 2H), 7.46 (s, 1H), 7.42-7.34 (m, 4H), 7.31 (d, $J = 3.1$ Hz, 1H), 7.11 (dd, $J = 10.4, 7.7$ Hz, 3H), 7.05 (dd, $J = 13.9, 8.4$ Hz, 2H), 6.98 (d, $J = 7.4$ Hz, 1H), 6.92 (t, $J = 7.6$ Hz, 1H), 6.37 (d, $J = 3.1$ Hz, 1H), 5.69 (dd, $J = 12.1, 5.4$ Hz, 1H), 3.98 (dd, $J = 17.6, 12.2$ Hz, 1H), 3.82 (s, 3H), 3.80 (s, 3H), 3.74 (s, 3H), 3.21 (dd, $J = 17.6, 5.4$ Hz, 1H). ^{13}C NMR (151 MHz, DMSO- d_6) δ 164.87, 159.91, 151.28, 149.54, 146.69, 136.28, 132.98, 130.77, 130.29, 129.12, 128.65, 127.74, 125.37, 123.93, 123.84, 120.62, 119.29, 118.99, 117.84, 115.57, 112.61, 111.58, 111.23, 111.00, 100.84, 63.60, 56.13, 55.64, 43.98, 32.97. HRMS (ESI-TOF) Calcd. for $\text{C}_{33}\text{H}_{30}\text{N}_4\text{O}_3$ $[\text{M}+\text{H}]^+$ 530.2451; Found 530.2450.

N-(3-bromophenyl)-4-(3-(3-methoxyphenyl)-5-(1-methyl-1*H*-indol-5-yl)-4,5-dihydro-1*H*-pyrazol-1-yl)benzamide (**Q13**)

Yellow solid, yield: 79.2%, m.p. 135-142 °C ^1H NMR (600 MHz, DMSO- d_6) δ 10.00 (s, 1H), 8.11 (d, $J = 55.5$ Hz, 1H), 8.02 (d, $J = 9.4$ Hz, 1H), 7.76 (d, $J = 8.8$ Hz, 1H), 7.62 (t, $J = 8.0$ Hz, 1H), 7.53-7.48 (m, 1H), 7.44 (t, $J = 7.4$ Hz, 2H), 7.39 (t, $J = 7.7$ Hz, 2H), 7.37-7.21 (m, 4H), 7.13 (d, $J = 8.7$ Hz, 1H), 7.07 (ddd, $J = 8.6, 3.8, 1.8$ Hz, 1H), 7.05-6.95 (m, 1H), 6.38 (ddd, $J = 11.0, 3.1, 0.8$ Hz, 1H), 5.77 (ddd, $J = 72.1, 12.1, 5.0$ Hz, 1H), 4.02 (ddd, $J = 41.7, 17.8, 12.1$ Hz, 1H), 3.83 (d, $J = 5.2$ Hz, 3H), 3.75 (d, $J = 7.8$ Hz, 3H), 3.27 (ddd, $J = 43.9, 17.7, 5.0$ Hz, 1H). ^{13}C NMR (151 MHz, DMSO- d_6) δ 165.77, 159.95, 152.48, 149.23, 143.22, 136.35, 133.88, 132.85, 130.97, 129.49, 129.06, 128.68, 125.68, 124.88, 123.01, 122.63, 120.28, 119.17, 117.73, 116.25, 115.54, 113.18, 112.51, 111.72, 111.00, 109.80, 100.90, 63.21, 55.72, 44.12, 32.97. HRMS (ESI-TOF) Calcd. for $\text{C}_{32}\text{H}_{27}\text{BrN}_4\text{O}_2$ $[\text{M}+\text{H}]^+$ 578.1347; Found

578.1346.

N-(4-chlorophenyl)-4-(3-(3-methoxyphenyl)-5-(1-methyl-1*H*-indol-5-yl)-4,5-dihydro-1*H*-pyrazol-1-yl)benzamide (**Q14**)

Yellow solid, yield: 74.3%, m.p. 135-142 °C ¹H NMR (600 MHz, DMSO-*d*₆) δ 8.14 (d, *J* = 8.5 Hz, 1H), 8.02 (d, *J* = 9.3 Hz, 2H), 7.81 (d, *J* = 8.4 Hz, 1H), 7.62 (t, *J* = 7.6 Hz, 1H), 7.51 (ddd, *J* = 8.2, 7.0, 1.0 Hz, 1H), 7.46 (d, *J* = 1.7 Hz, 1H), 7.45-7.42 (m, 2H), 7.43-7.37 (m, 3H), 7.33 (d, *J* = 3.1 Hz, 1H), 7.26 (s, 1H), 7.07 (dd, *J* = 8.5, 1.8 Hz, 1H), 7.04 (ddd, *J* = 8.1, 2.6, 1.1 Hz, 1H), 6.39 (dd, *J* = 3.1, 0.8 Hz, 1H), 5.84 (dd, *J* = 11.9, 4.6 Hz, 1H), 4.06 (dd, *J* = 17.9, 11.9 Hz, 1H), 3.83 (d, *J* = 9.5 Hz, 3H), 3.75 (d, *J* = 9.8 Hz, 3H), 3.30 (dd, *J* = 17.9, 4.6 Hz, 1H). ¹³C NMR (151 MHz, DMSO-*d*₆) δ 167.69, 159.90, 149.95, 147.48, 133.81, 132.91, 131.18, 130.78, 130.29, 128.63, 120.11, 119.22, 119.04, 117.72, 115.68, 112.50, 111.26, 111.00, 100.84, 63.46, 55.65, 44.03, 32.96. HRMS (ESI-TOF) Calcd. for C₃₂H₂₇ClN₄O₂ [M+H]⁺ 534.1894; Found 534.1892.

N-(4-fluorophenyl)-4-(3-(3-methoxyphenyl)-5-(1-methyl-1*H*-indol-5-yl)-4,5-dihydro-1*H*-pyrazol-1-yl)benzamide (**Q15**)

White solid, yield: 80.2%, m.p. 129-137 °C ¹H NMR (600 MHz, DMSO-*d*₆) δ 9.71 (s, 1H), 8.14 (d, *J* = 8.4 Hz, 1H), 8.02 (s, 1H), 8.01 (s, 1H), 7.79 (dd, *J* = 17.5, 8.7 Hz, 1H), 7.62 (t, *J* = 7.6 Hz, 1H), 7.50 (dd, *J* = 16.3, 8.2 Hz, 2H), 7.47-7.35 (m, 5H), 7.33 (d, *J* = 3.1 Hz, 1H), 7.26 (s, 1H), 7.07 (dd, *J* = 8.5, 1.7 Hz, 1H), 7.04 (dd, *J* = 7.6, 2.2 Hz, 1H), 6.39 (d, *J* = 3.0 Hz, 1H), 5.83 (dd, *J* = 11.9, 4.6 Hz, 1H), 4.06 (dd, *J* = 17.9, 12.0 Hz, 1H), 3.84 (s, 3H), 3.76 (s, 3H), 3.30 (dd, *J* = 17.9, 4.6 Hz, 1H). ¹³C

NMR (151 MHz, DMSO- d_6) δ 158.87, 151.38, 148.15, 142.15, 135.28, 132.28, 131.76, 129.83, 129.32, 128.47, 127.93, 124.59, 119.20, 118.31, 118.09, 116.67, 115.16, 112.10, 111.44, 110.65, 110.05, 108.71, 99.83, 62.15, 54.63, 43.04, 31.91.

HRMS (ESI-TOF) Calcd. for C₃₂H₂₇N₄O₂ [M+H]⁺ 518.2189; Found 518.2188.

4-(3-(3-methoxyphenyl)-5-(1-methyl-1*H*-indol-5-yl)-4,5-dihydro-1*H*-pyrazol-1-yl)-*N*-(*o*-tolyl)benzamide (**Q16**)

Yellow solid, yield: 70.5%, m.p. 130-144 °C. ¹H NMR (600 MHz, DMSO- d_6) δ 10.13 (s, 1H), 8.14 (dd, J = 8.8, 5.7 Hz, 2H), 8.00 (d, J = 9.4 Hz, 2H), 7.81 (dd, J = 8.8, 3.3 Hz, 3H), 7.61 (t, J = 7.7 Hz, 1H), 7.51 (t, J = 7.2 Hz, 1H), 7.46-7.42 (m, 3H), 7.33 (d, J = 3.1 Hz, 1H), 7.07 (dd, J = 8.5, 1.8 Hz, 1H), 7.05 (d, J = 2.3 Hz, 1H), 7.03 (d, J = 2.6 Hz, 1H), 6.39 (dd, J = 3.0, 0.8 Hz, 1H), 5.79 (dd, J = 11.8, 4.5 Hz, 1H), 4.04 (dd, J = 17.8, 11.8 Hz, 1H), 3.82 (s, 3H), 3.80 (s, 3H), 3.76 (s, 3H), 3.26 (dd, J = 17.8, 4.5 Hz, 1H). ¹³C NMR (151 MHz, DMSO- d_6) δ 161.79, 158.82, 151.39, 148.14, 145.48, 142.14, 135.18, 132.83, 131.21, 129.70, 128.47, 127.92, 125.77, 124.90, 123.79, 119.19, 118.08, 117.88, 116.65, 115.16, 114.41, 112.09, 111.44, 110.64, 108.71, 99.82, 99.75, 62.49, 54.57, 31.89, 17.33. HRMS (ESI-TOF) Calcd. for C₃₃H₃₀N₄O₂ [M+H]⁺ 514.2495; Found 514.2495.

N-(3,4-dichlorophenyl)-4-(3-(3-methoxyphenyl)-5-(1-methyl-1*H*-indol-5-yl)-4,5-dihydro-1*H*-pyrazol-1-yl)benzamide (**Q17**)

White solid, yield: 93.3%, m.p. 100-112 °C. ¹H NMR (600 MHz, DMSO- d_6) δ 8.14 (d, J = 8.4 Hz, 1H), 8.02 (d, J = 8.9 Hz, 2H), 7.81 (d, J = 8.3 Hz, 1H), 7.62 (t, J = 7.4 Hz, 1H), 7.51 (t, J = 7.7 Hz, 1H), 7.46 (s, 1H), 7.44 (t, J = 7.6 Hz, 2H), 7.41-7.38

(m, 2H), 7.33 (d, $J = 3.1$ Hz, 1H), 7.26 (s, 1H), 7.07 (dd, $J = 8.5, 1.7$ Hz, 1H), 7.04 (dd, $J = 8.0, 2.5$ Hz, 1H), 6.39 (d, $J = 3.1$ Hz, 1H), 5.84 (dd, $J = 11.9, 4.6$ Hz, 1H), 4.06 (dd, $J = 17.9, 11.9$ Hz, 1H), 3.84 (s, 3H), 3.76 (s, 3H), 3.30 (dd, $J = 17.9, 4.6$ Hz, 1H). ^{13}C NMR (151 MHz, DMSO- d_6) δ 158.86, 151.39, 148.14, 142.14, 135.27, 132.28, 131.76, 129.83, 129.32, 128.47, 127.93, 127.60, 124.59, 119.19, 118.31, 118.09, 116.65, 115.17, 112.09, 110.64, 110.60, 110.05, 108.71, 99.82, 62.14, 54.63, 43.04, 31.91. HRMS (ESI-TOF) Calcd. for $\text{C}_{32}\text{H}_{26}\text{Cl}_2\text{N}_4\text{O}_2$ $[\text{M}+\text{H}]^+$ 568.1433; Found 568.1431.

4-(3-(3-methoxyphenyl)-5-(1-methyl-1*H*-indol-5-yl)-4,5-dihydro-1*H*-pyrazol-1-yl)-*N*-(4-nitrophenyl)benzamide (**Q18**)

White solid, yield: 75.5%, m.p. 105-110 °C. ^1H NMR (600 MHz, DMSO- d_6) δ 8.14 (d, $J = 8.4$ Hz, 1H), 8.02 (d, $J = 9.3$ Hz, 2H), 7.81 (d, $J = 8.4$ Hz, 2H), 7.62 (t, $J = 7.6$ Hz, 1H), 7.51 (t, $J = 7.4$ Hz, 1H), 7.46 (s, 1H), 7.44 (t, $J = 7.0$ Hz, 1H), 7.42-7.38 (m, 3H), 7.33 (d, $J = 3.1$ Hz, 1H), 7.26 (s, 1H), 7.07 (dd, $J = 8.5, 1.7$ Hz, 1H), 7.04 (dd, $J = 8.1, 2.7$ Hz, 1H), 6.39 (d, $J = 3.1$ Hz, 1H), 5.84 (dd, $J = 12.0, 4.6$ Hz, 1H), 4.06 (dd, $J = 17.9, 11.9$ Hz, 1H), 3.84 (s, 3H), 3.76 (s, 3H), 3.30 (dd, $J = 17.9, 4.6$ Hz, 1H). ^{13}C NMR (151 MHz, DMSO- d_6) δ 159.94, 152.48, 149.22, 143.22, 136.35, 133.36, 132.84, 132.29, 130.91, 130.40, 129.56, 128.68, 125.68, 120.27, 119.39, 119.17, 117.73, 116.25, 113.17, 111.72, 111.68, 111.13, 109.80, 100.90, 63.21, 55.72, 44.12, 33.00. HRMS (ESI-TOF) Calcd. for $\text{C}_{32}\text{H}_{27}\text{N}_5\text{O}_4$ $[\text{M}+\text{H}]^+$ 545.2179; Found 545.2178.

N-(3,5-bis(trifluoromethyl)phenyl)-4-(3-(3-methoxyphenyl)-5-(1-methyl-1*H*-indol-5-

yl)-4,5-dihydro-1*H*-pyrazol-1-yl)benzamide (**Q19**)

White solid, yield: 80.4%, m.p. 138-147 °C. ¹H NMR (600 MHz, DMSO-*d*₆) δ 8.14 (d, *J* = 8.4 Hz, 1H), 8.02 (d, *J* = 8.8 Hz, 2H), 7.81 (d, *J* = 8.3 Hz, 1H), 7.62 (t, *J* = 7.7 Hz, 1H), 7.51 (t, *J* = 7.0 Hz, 1H), 7.46 (s, 1H), 7.44 (t, *J* = 7.1 Hz, 2H), 7.41-7.38 (m, 2H), 7.33 (d, *J* = 3.0 Hz, 1H), 7.26 (s, 1H), 7.07 (d, *J* = 8.2 Hz, 1H), 7.04 (dd, *J* = 8.1, 2.3 Hz, 1H), 6.39 (d, *J* = 3.1 Hz, 1H), 5.84 (dd, *J* = 11.9, 4.6 Hz, 1H), 4.06 (dd, *J* = 17.9, 11.9 Hz, 1H), 3.84 (s, 3H), 3.76 (s, 3H), 3.30 (dd, *J* = 17.9, 4.6 Hz, 1H). ¹³C NMR (151 MHz, DMSO-*d*₆) δ 131.10, 117.43, 116.00, 111.44, 109.40, 108.05, 99.17, 61.49, 53.97, 42.38, 38.76, 38.64, 38.62, 38.50, 38.37, 38.23, 38.09, 37.95, 37.81, 31.25. HRMS (ESI-TOF) Calcd. for C₃₄H₂₆F₆N₄O₂ [M+H]⁺ 636.2058; Found 636.2056.

N-(3,4-difluorophenyl)-4-(3-(3-methoxyphenyl)-5-(1-methyl-1*H*-indol-5-yl)-4,5-dihydro-1*H*-pyrazol-1-yl)benzamide (**Q20**)

White solid, yield: 85.7%, m.p. 125-140 °C. ¹H NMR (600 MHz, DMSO-*d*₆) δ 8.14 (d, *J* = 8.5 Hz, 1H), 8.02 (d, *J* = 9.2 Hz, 2H), 7.81 (d, *J* = 8.4 Hz, 1H), 7.62 (t, *J* = 7.8 Hz, 1H), 7.51 (t, *J* = 7.7 Hz, 1H), 7.47 (s, 1H), 7.44 (t, *J* = 7.3 Hz, 2H), 7.41-7.38 (m, 2H), 7.33 (d, *J* = 3.1 Hz, 1H), 7.26 (s, 1H), 7.07 (d, *J* = 7.0 Hz, 1H), 7.04 (dd, *J* = 7.8, 2.1 Hz, 1H), 6.39 (d, *J* = 2.9 Hz, 1H), 5.83 (dd, *J* = 11.9, 4.6 Hz, 1H), 4.06 (dd, *J* = 17.9, 11.9 Hz, 1H), 3.83 (d, *J* = 9.4 Hz, 3H), 3.75 (d, *J* = 9.8 Hz, 3H), 3.30 (dd, *J* = 17.9, 4.6 Hz, 1H). ¹³C NMR (151 MHz, DMSO-*d*₆) δ 157.47, 149.96, 146.75, 140.77, 130.89, 130.34, 128.43, 127.91, 127.05, 123.18, 117.80, 116.91, 116.69, 115.29, 113.74, 110.70, 109.26, 109.22, 108.65, 107.29, 98.44, 60.78, 53.22, 41.64, 30.51.

HRMS (ESI-TOF) Calcd. for $C_{32}H_{26}F_2N_4O_2$ $[M+H]^+$ 536.2082; Found 536.2081.

4.3. Anti-proliferative assay

Five cancer cell lines, HCT116, SW480, HT29 (human colorectal cell lines), CT26 (mice colorectal cell lines), HeLa (human cervix cell line), and one noncancer cell line, 293T (human embryonic kidney cell line) were used in the evaluation of antiproliferation activities with a standard MTT-based colorimetric assay. The cells were seeded at a density of 5×10^4 /well into 96-well plates and incubated for 12 h at 37 °C, 5% CO₂ atmosphere. Experimental groups were treated with concentrations of synthesized compounds and Regorafenib was used as the positive control. MTT was applied to check the status of the cells after 48 h. The absorbance (OD 570 nm) was read on an ELISA reader (ELx800, BioTek, USA) with reference wavelength of 630 nm. Then the GI₅₀ values were calculated.

4.4. Inhibitory activity upon APC-Asef interactions

We used the previously established fluorescence polarization immunoassay to evaluate the inhibitory activity upon APC-Asef interactions [34,35]. The proteins and corresponding anti-bodies were purchased as mentioned in the materials. The concentrations of APC and Asef were set as 1 mM when the stock solution was prepared. Along with the diluting of Asef solution, the concentrations of Corning NBS 3995 were set in the gradient of 1, 0.1, 0.01 and 0.001 mM. After adding APC, the mixture was incubated at room temperature for 2 h. Then tested compounds were added at various concentrations. After a further incubation for 2 h, the fluorescent signals at 525 nm were read with the excitation wavelength of 480 nm. Then, the IC₅₀

values were calculated accordingly.

4.5. Cell apoptosis assay

HCT116 cells were seeded in six-well plates at the density of 2×10^5 /well, and treated with compound **Q19** at final concentrations of 0, 0.2, 0.5, 1.0, 2.0 and 5.0 μM for 24 h to induce cell apoptosis. Then the cells were harvested and washed twice with ice-cold PBS. After being resuspended by binding buffer, the cells were incubated with Annexin-V/FITC (5 mL) and PI (5 mL) for a further 10 min in the dark. The same protocol was also used for HT29. We used a flow-cytometer (Becton Dickinson, USA) to analyze the result and conducted the statistical analysis with Flowjo 7.6.1 software.

4.6. Mitochondrial membrane potential assay

Mitochondrial transmembrane potential was detected with a JC-1 mitochondrial membrane potential assay kit (Beyotime Biotech). After the incubation with 5 $\mu\text{g/mL}$ JC-1 at 37 °C for 20 min, the cells were washed twice with PBS and placed in fresh medium without serum. The samples were analyzed using a FACSCalibur cytometer (Becton Dickinson) at 488 nm.

4.7. Molecular docking simulation

The crystal structures of APC protein (PDB Code: 3NMX) was retrieved from the RCSB Protein Data Bank (<http://www.rcsb.org>). After a procedure of eliminating water and adding polar hydrogen, the protein was well prepared. Molecular docking of all compounds was then carried out using the Discovery Studio (version 3.5) as implemented through the graphical user interface CDOCKER protocol, which was an

implementation of a CHARMM based molecular docking tool using a half-flexible receptor.

Supporting Information

NMR spectra were detailed in the Supporting Information. Supporting Information associated with this article can be found, in the online version, at <http://dx.doi.org/10.1016/j.XXX.2019.XX.XXX>.

Acknowledgments

This work is supported by the National Undergraduate Innovation Program and the National Science Foundation of China (No. S201910284029).

Declaration of Competing Interest

The authors have no conflict of interests to declare.

References

- [1] L. Vanaelst, M. Barr, S. Marcus, A. Polverino, M. Wigler, Complex-formation between Ras and Raf and other protein-kinases, *Proc. Natl. Acad. Sci. U.S.A.* 90 (1993) 6213-6217.
- [2] H. Chong, H. G. Vikis, K. L. Guan, Mechanisms of regulating the Raf kinase family, *Cell. Signal.* 15 (2003) 463-469.
- [3] P. Chene, Inhibiting the p53-MDM2 interaction: An important target for cancer therapy, *Nat. Rev. Cancer* 3 (2003) 102-109.
- [4] O. Vanunu, O. Magger, E. Ruppin, T. Shlomi, R. Sharan, Associating genes and

protein complexes with disease via network propagation, *PLoS Comput. Biol.* 6 (2010) e1000641.

[5] J. Roos, S. Grosch, O. Werz, P. Schroder, S. Ziegler, S. Fulda, P. Paulus, A. Urbschat, B. Kuhn, I. Maucher, J. Fettel, T. Vorup-Jensen, M. Piesche, C. Matrone, D. Steinhilber, M. J. Parnham, T. J. Maier, Regulation of tumorigenic Wnt signaling by cyclooxygenase-2, 5-lipoxygenase and their pharmacological inhibitors: A basis for novel drugs targeting cancer cells? *Pharmacol. Therapeut.* 157 (2016) 43-64.

[6] L. Dong, L. Y. Wang, L. M. Sui, H. Y. Zhao, X. X. Xu, T. Y. Li, X. N. Wang, W. J. Li, P. Zhou, L. Kong, Claudin-7 indirectly regulates the integrin/FAK signaling pathway in human colon cancer tissue, *J. Hum. Genet.* 61 (2016) 711-720.

[7] T. Akiyama, Y. Kawasaki, Wnt signalling and the actin cytoskeleton, *Oncogene* 25 (2006) 7538-7544.

[8] J. Schneikert, J. Behrens, The canonical Wnt signalling pathway and its APC partner in colon cancer development, *Gut* 56 (2007) 417-425.

[9] K. Aoki, M. M. Taketo, Adenomatous polyposis coli (APC): a multi-functional tumor suppressor gene, *J. Cell Sci.* 120 (2007) 3327-3335.

[10] Y. Kawasaki, T. Jigami, S. Furukawa, M. Sagara, K. Echizen, Y. Shibata, R. Sato, T. Akiyama, The adenomatous polyposis coli-associated guanine nucleotide exchange factor Asef is involved in angiogenesis, *J. Biol. Chem.* 285 (2010) 1199-1207.

[11] S. Futaki, Membrane-permeable arginine-rich peptides and the translocation mechanisms, *Adv. Drug Deliv. Rev.* 57 (2005) 547-558.

- [12] M. Vedadi, F. H. Niesen, A. Allali-Hassani, O. Y. Fedorov, P. J. Finerty, G. A. Wasney, R. Yeung, C. Arrowsmith, L. J. Ball, H. Berglund, R. Hui, B. D. Marsden, P. Nordlund, M. Sundstrom, J. Weigelt, A. M. Edwards, Chemical screening methods to identify ligands that promote protein stability, protein crystallization, and structure determination, *Proc. Natl. Acad. Sci. U.S.A.* 103 (2006) 15835-15840.
- [13] F. H. Niesen, H. Berglund, M. Vedadi, The use of differential scanning fluorimetry to detect ligand interactions that promote protein stability, *Nat. Protoc.* 2 (2007) 2212-2221.
- [14] N. Qvit, S. J. S. Rubin, T. J. Urban, D. Mochly-Rosen, E. R. Gross, Peptidomimetic therapeutics: scientific approaches and opportunities, *Drug Discov. Today* 22 (2017) 454-462.
- [15] R. Fodde, R. Smith, H. Clevers, APC, signal transduction and genetic instability in colorectal cancer, *Nat. Rev. Cancer* 1 (2001) 55-67.
- [16] K. B. Kaplan, A. A. Burds, J. R. Swedlow, S. S. Bekir, P. K. Sorger, I. S. Nathke, A role for the Adenomatous Polyposis Coli protein in chromosome segregation, *Nat. Cell Biol.* 3 (2001) 429-432.
- [17] E. C. Morishita, K. Murayama, M. Kato-Murayama, Y. Ishizuka-Katsura, Y. Tomabechi, T. Hayashi, T. Terada, N. Handa, M. Shirouzu, T. Akiyama, S. Yokoyama, Crystal structures of the armadillo repeat domain of adenomatous polyposis coli and its complex with the tyrosine-rich domain of Sam68, *Structure* 19 (2011) 1496-1508.
- [18] D. M. Molina, R. Jafari, M. Ignatushchenko, T. Seki, E. A. Larsson, C. Dan, L.

Sreekumar, Y. Cao, P. Nordlund, Monitoring drug target engagement in cells and tissues using the cellular thermal shift assay, *Science* 341 (2013) 84-87.

[19] D. Martinez Molina, P. Nordlund, The cellular thermal shift assay: a novel biophysical assay for in situ drug target engagement and mechanistic biomarker studies, *Annu. Rev. Pharmacol. Toxicol.* 56 (2016) 141-161.

[20] H. Almqvist, H. Axelsson, R. Jafari, C. Dan, A. Mateus, M. Haraldsson, A. Larsson, D. M. Molina, P. Artursson, T. Lundback, P. Nordlund, CETSA screening identifies known and novel thymidylate synthase inhibitors and slow intracellular activation of 5-fluorouracil, *Nat. Commun.* 7 (2016) 11040.

[21] K. F. Ding, L. F. Sun, W. T. Ge, H. G. Hu, S. Z. Zhang, S. Zheng, Effect of SNC19/ST14 gene overexpression on invasion of colorectal cancer cells, *World J. Gastroenterol.* 11 (2005) 5651-5654.

[22] M. J. Hamann, C. M. Lubking, D. N. Luchini, D. D. Billadeau, Asef2 functions as a Cdc42 exchange factor and is stimulated by the release of an autoinhibitory module from a concealed C-terminal activation element, *Mol. Cell. Biol.* 27 (2007) 1380-1393.

[23] O. Sbai, T. S. Devi, M. A. B. Melone, F. Feron, M. Khrestchatisky, L. P. Singh, L. Perrone, RAGE-TXNIP axis is required for S100B-promoted Schwann cell migration, fibronectin expression and cytokine secretion, *J. Cell Sci.* 123 (2010) 4332-4339.

[24] S. Diemert, A. M. Dolga, S. Tobaben, J. Grohm, S. Pfeifer, E. Oexler, C. Culmsee, Impedance measurement for real time detection of neuronal cell death, *J.*

Neurosci. Methods 203 (2012) 69-77.

[25] S. M. Farrington, M. G. Dunlop, Mosaicism and sporadic familial adenomatous polyposis, *Am. J. Hum. Genet.* 64 (1999) 653-658.

[26] A. S. Ripka, D. H. Rich, Peptidomimetic design, *Curr. Opin. Chem. Biol.* 2 (1998) 441-452.

[27] S. A. Macnab, S. J. Turrell, I. M. Carr, A. F. Markham, P. L. Coletta, A. Whitehouse, Herpesvirus saimiri-mediated delivery of the adenomatous polyposis coli tumour suppressor gene reduces proliferation of colorectal cancer cells, *Int. J. Oncol.* 39 (2011) 1173-1181.

[28] C. L. Floquet, J. P. Rousset, L. Bidou, Readthrough of premature termination codons in the adenomatous polyposis coli gene restores its biological activity in human cancer cells, *PLoS One* 6 (2011), e24125.

[29] K. Fosgerau, T. Hoffmann, Peptide therapeutics: current status and future directions, *Drug Discov. Today* 20 (2015) 122-128.

[30] M. Pelay-Gimeno, A. Glas, O. Koch, T. N. Grossmann, Grossmann, Structurebased design of inhibitors of protein-protein interactions: mimicking peptide binding epitopes, *Angew. Chem., Int. Ed. Engl.* 54 (2015) 8896-8927.

[31] X. Zhao, Y. Wang, R. Deng, H. Zhang, J. Dou, H. Yuan, G. Hou, Y. Du, Q. Chen, J. Yu, miR186 suppresses prostate cancer progression by targeting Twist1, *Oncotarget* 7 (2016) 33136-33151.

[32] H. M. Jiang, R. Deng, X. Y. Yang, J. L. Shang, S. Y. Lu, Y. L. Zhao, K. Song, X. Y. Liu, Q. F. Zhang, Y. Chen, Y. E. Chinn, G. Wu, J. Li, G. Q. Chen, J. X. Yu, J.

Zhang, Peptidomimetic inhibitors of APC-Asef interaction block colorectal cancer migration, *Nat. Chem. Biol.* 13 (2017) 994-1001.

[33] X. Y. Yang, J. Zhong, Q. F. Zhang, J. X. Qian, K. Song, C. Ruan, J. R. Xu, K. Ding, J. Zhang, Rational design and structure validation of a novel peptide inhibitor of the Adenomatous-Polyposis-Coli (APC)-Rho-Guanine-Nucleotide-Exchange-Factor-4 (Asef) interaction, *J. Med. Chem.* 61 (2018) 8017-8028.

[34] X. Q. Yan, Z. C. Wang, P. F. Qi, G. G. Li, H. L. Zhu, Design, synthesis and biological evaluation of 2-H pyrazole derivatives containing morpholine moieties as highly potent small molecule inhibitors of APC-Asef interaction, *Eur. J. Med. Chem.* 177 (2019) 425-447.

[35] Z. Nikolovska-Coleska, R. Wang, X. Fang, H. Pan, Y. Tomita, P. Li, P. P. Roller, K. Krajewski, N. G. Saito, J. A. Stuckey, S. Wang, Development and optimization of a binding assay for the XIAP BIR3 domain using fluorescence polarization, *Anal. Biochem.* 332 (2004) 261-273.

[36] W. J. Egan, G. Lauri, Prediction of intestinal permeability. *Adv Drug Del. Rev.* 54 (2002) 273-289.

Discovery of novel pyrazoline derivatives containing methyl-1*H*-indole moiety as potential inhibitors for blocking APC-Asef interactions

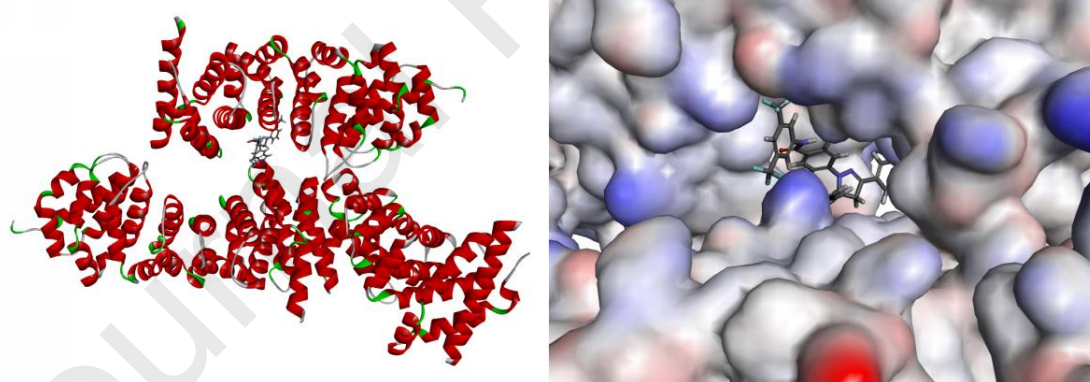
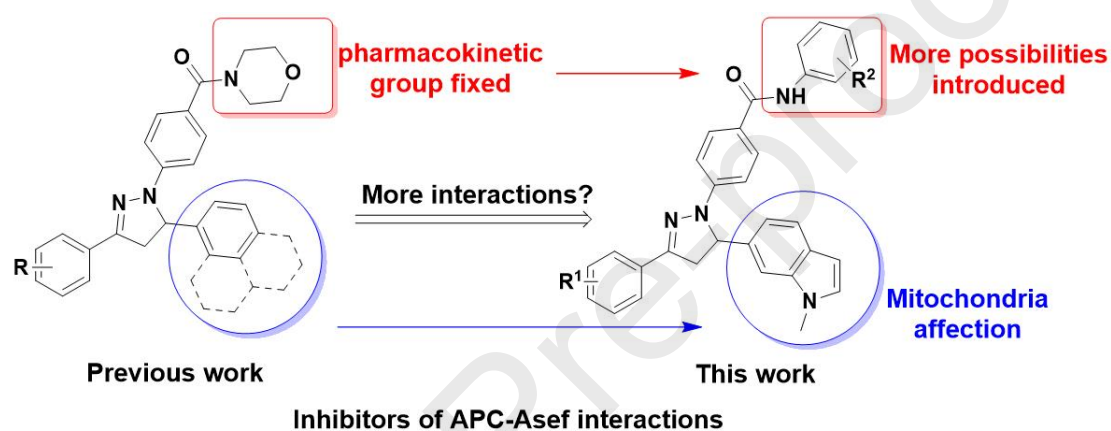
Peng-Fei Qi,[†] Li Fang,[†] Hua Li, Shu-Kai Li, Yu-Shun Yang, Jin-Liang Qi,^{*} Chen Xu,^{*} and

Hai-Liang Zhu^{*}

State Key Laboratory of Pharmaceutical Biotechnology, Nanjing University, Nanjing 210023, China

[†]Both authors contributed equally to the work

^{*}Corresponding author. Tel. & Fax: +86-25-89682672; E-mail: zhuhl@nju.edu.cn; xuchn@nju.edu.cn; QiJL@nju.edu.cn.



A series of novel pyrazoline derivatives containing methyl-1*H*-indole moiety were discovered as potential inhibitors for blocking APC-Asef interactions. The top hit **Q19** suggested potency of inhibiting APC-Asef interactions and attractive preference for human-sourced colorectal cells. The introduction of methyl-1*H*-indole moiety realized the Mitochondrial affection, connecting the impact on the protein-interaction level with the apoptosis events. This work raised referable information for further discovery of inhibitors for blocking APC-Asef interactions.

- > Providing a novel series of potential inhibitors for blocking APC-Asef interactions
- > The series **Q1-Q20** were all reported for the first time
- > The top hit **Q19** suggested potency of inhibiting APC-Asef interactions and attractive preference for human-sourced colorectal cells
- > The introduction of methyl-1*H*-indole moiety realized the Mitochondrial affection, connecting the impact on the protein-interaction level with the apoptosis events

Conflict of Interest Statements for Authors:

All authors declare that there are no conflicts of interest.

Journal Pre-proofs